Biophysical characterization and structure of the Fab fragment from the NIST reference antibody, RM 8671

Ioannis Karageorgos [a, b], Elyssia S. Gallagher [a, b, 1], Connor Galvin [a, b], D. Travis Gallagher [a, b, **], Jeffrey W. Hudgens [a, b, *]

[a] Biomolecular Measurement Division, National Institute of Standards & Technology, Rockville, MD 20850, USA
[b] Institute for Bioscience and Biotechnology Research, 9600 Gudelsky Drive, Rockville, MD 20850, USA

ABSTRACT

Monoclonal antibody pharmaceuticals are the fastest-growing class of therapeutics, with a wide range of clinical applications. To assure their safety, these protein drugs must demonstrate highly consistent purity and stability. Key to these objectives is higher order structure measurements validated by calibration to reference materials. We describe preparation, characterization, and crystal structure of the Fab fragment prepared from the NIST Reference Antibody RM 8671 (NISTmAb). NISTmAb is a humanized IgG1κ antibody, produced in murine cell culture and purified by standard biopharmaceutical production methods, developed at the National Institute of Standards and Technology (NIST) to serve as a reference material. The Fab fragment was derived from NISTmAb through papain cleavage followed by protein A based purification. The purified Fab fragment was characterized by SDS-PAGE, capillary gel electrophoresis, multi-angle light scattering, size exclusion chromatography, mass spectrometry, and x-ray crystallography. The crystal structure at 0.2 nm resolution includes four independent Fab molecules with complete light chains and heavy chains through Cys 223, enabling assessment of conformational variability and providing a well-characterized reference structure for research and engineering applications. This nonproprietary, publically available reference material of known higher-order structure can support metrology in biopharmaceutical applications, and it is a suitable platform for validation of molecular modeling studies.

Published by Elsevier Ltd on behalf of International Alliance for Biological Standardization.

1. Introduction

The number of FDA-approved monoclonal antibody (mAb) pharmaceuticals has increased exponentially since 2000, doubling every four years, and now numbers about 60. Global sales of monoclonal antibody pharmaceuticals in 2016 were $105B, comprising greater than ten metric tons of material [1,2]. The mAb drugs demonstrate a trend toward smarter, more specific, and hence, safer therapeutics. Their production also reflects a

significant investment since mAbs are among the greatest molecular weight, complex therapeutics ever produced. Part of the price for their etiologic specificity is that their production, requiring cultured mammalian cells, is highly elaborate, and the proteins themselves are relatively heterogeneous and sensitive to their physical environment [3]. Since their clinical efficacy depends on their biophysical properties, in particular the higher order structure, it is necessary to measure those properties repeatedly and consistently. Therefore, a well-characterized mAb reference material that can facilitate development of improved analytical tools and computational simulations, particularly for characterization of higher order structure, will help assure the continued improvement of mAb biotherapeutics.

Reference materials reside at the heart of monoclonal antibody production to assure consistent product properties and quality over the lifetime of the therapeutic protein. The National Institute of Standards and Technology (NIST) has introduced a IgG1κ antibody reference material, NISTmAb (RM 8671) [4,5], as part of a program

* Corresponding author. Biomolecular Measurement Division, National Institute of Standards & Technology, Rockville, MD 20850, USA.
** Corresponding author.Biomolecular Measurement Division, National Institute of Standards & Technology, Rockville, MD 20850, USA.
E-mail addresses: Ioannis.Karageorgos@nist.gov (I. Karageorgos), Elyssia_Gallagher@baylor.edu (E.S. Gallagher), travis.gallagher@nist.gov (D.T. Gallagher), jeffrey.hudgens@nist.gov (J.W. Hudgens).
1 Current address: Department of Chemistry and Biochemistry, Baylor University, One Bear Place #97348, Waco, TX, 76798.

to develop fundamental materials and data in support of the bio-pharmaceutical industry. To support the utility of this reference material, it was characterized by over twenty-four analytical methods and the results from these studies are presented in three volumes [6–8]. Those volumes focus on the mAb and do not include crystal structures for NISTmAb or its Fab fragment.

Here we report the preparation, biophysical characterization, and x-ray crystal structure of the Fab fragment derived from NISTmAb material RM 8671. Mass spectrometry indicates that heavy chain cleavage by papain occurred after His 227. The crystal structure is generally representative of the Protein Data Bank's repertoire of about 500 human and humanized Fab structures [9]. However, the structure is more complete (in particular, including the entire light chain and all 5 disulfides per Fab) and includes four independent Fab fragments, thus providing information on structural variability. The structure reported here is of the Fab fragment in its ligand-free (apo) state, enabling comparison with the previously published Fab complex (holo) structure [10] and inferences on complementarity determining region (CDR) mobility. The structure provides reproducible reference data to support comparisons over time and across Fab-related projects in research and molecular engineering.

2. Materials and methods

2.1. Preparation of Fab fragment

Fab fragment production by cleavage of mAbs using papain, followed by protein A has become routine, such that several commercial kits are available, using agarose-immobilized forms of the peptidase (extracted from papaya fruit latex) and protein A (from *Staph. aureus*, recombinantly expressed in *E. coli*) [11]. Papain's broad specificity enables it to cleave all 4 subclasses of human IgG in the hinge region, despite their different hinge sequences. Cleavage efficiencies correlate with hinge lengths (IgG3 >> IgG1 > IgG2 ~ IgG4) and are generally enhanced by reducing agent, suggesting that accessibility of the hinge to the 23 kDa enzyme is the key to cleavage [12]. For this study NISTmAb, produced in murine cell culture, was treated by the components of the Pierce Fab Preparation kit (Model 44985, Thermo Scientific, Waltham, MA) to produce the Fab fragment. This method uses immobilized papain for cleavage and immobilized protein A to isolate the Fab fragment. For a small-scale preparation, 4 mg of NISTmAb in 0.5 mL of 20 mmol/L L-histidine, pH 6.0, were pre-equilibrated in cleavage buffer using a Zeba spin desalting column and then incubated with 0.25 mL (50% slurry) preequilibrated immobilized papain under mixing for 5 h at 37 °C. The digest was separated from papain by centrifugation (5000 g for 1 min). Papain was washed with 0.5 mL sodium phosphate buffered saline (PBS) solution (pH 7.4) for complete recovery of the digest. The digest was then applied to a PBS-equilibrated NAb column (protein A agarose) and incubated at room temperature for 10 min with agitation to capture the Fc and undigested NISTmAb. Fab fragment was then collected as the supernatant after centrifugation at 1000g for 1 min. Half of the Fab fragment was dialyzed in 10 mmol/L disodium phosphate, 10 mmol/L monosodium phosphate, 150 mmol/L sodium chloride, pH 7.4, and the other half in 100 mmol/L ammonium acetate, pH 6.0. For preparations of Fab from NISTmAb the typical yield is 55%.

2.2. Size exclusion chromatography

200 μL 100 μmol/L filtered Fab protein was applied to a GE Healthcare Superdex 75 10/300 GL column (GE Healthcare Bio-Sciences, Pittsburgh, PA), which was previously calibrated and equilibrated on an ÄKTAPurifier system (Amersham Pharmacia

Biotechnology, Amersham, UK). (Note: In this text all references to filters refer to a 0.22 μm nominal pore size.) The dialyzed Fab samples, with 10 mmol/L disodium phosphate, 10 mmol/L mono-sodium phosphate, 150 mmol/L sodium chloride, pH 7.4, and 100 mmol/L ammonium acetate, pH 6.0, were monitored at 280 nm, and the elution volume was recorded for each peak.

2.3. SDS-PAGE

Protein samples and molecular mass markers (Bio-Rad Laboratories, Inc., Hercules, CA) were resolved on a 15% SDS-PAGE gel in reducing (incubated at 70 °C for 5 min in Laemni buffer (Sigma-Aldrich, Inc., St. Louis, MO) containing 5% β-mercaptoethanol (v/v)) and nonreducing (absence of β-mercaptoethanol) conditions. Gels were stained using Coomassie blue (Model 1610786, Bio-Rad, Hercules, CA) stain.

2.4. Capillary gel electrophoresis (CGE)

200 μg filtered Fab was mixed with 100 μL of SDS- sample buffer (100 mmol/L Tris − HCl, pH 9.0, 1% SDS) and 4 μL of a 10 kDa internal standard. Half of the sample has been treated with 5 μL β-mercaptoethanol to reduce disulfide bonds while the other half was used to conduct CGE in non-reduced conditions. Samples were centrifuged at 300 *g* for 1 min and heated at 70 °C for 10 min. A PA 800 Plus Pharmaceutical Analysis System (PA 80 Plus, Sciex) with PDA detection at 220 nm was used to analyze Fab in reduced and non-reduced conditions. For each separation cycle, the capillary was first preconditioned with 0.1 mmol/L NaOH, 0.1 mmol/L HCl, deionized water, and SDS gel buffer. Prior to use, all gel buffers were degassed for 2 min under vacuum. Samples were electrokinetically introduced by applying voltage at −5 kV for 20 s. Electrophoresis was performed at constant voltage with applied field strength of −497 V/cm with a capillary thermostatted to 25 °C, using recirculating liquid coolant.

2.5. Mass spectrometric analysis

To determine the molecular weight of the Fab fragment, an aliquot of intact desalted and filtered Fab was analyzed by an Agilent Infinity II UHPLC coupled with an Agilent 6545 (electrospray) Q-TOF mass spectrometer (Agilent Technologies, Santa Clara, CA). A Bio-Spin 6 column (Bio-Rad, Hercules, CA) with 50 mmol/L ammonium bicarbonate buffer, pH 7.4, was used for desalting Fab. The Fab (3 μg) was injected onto an Agilent PLRP-S Column (1 mm × 50 mm, 100 nm pore size, 5 μm particle size). The mobile phase comprised Solvent A consisting of 0.1% formic acid in water (v/v) and Solvent B consisting of 0.1% formic acid in acetonitrile (v/v). After desalting by flowing a mixture of 80% Solvent A and 20% Solvent B through the column for 2 min at 0.4 mL/min, the sample was eluted from the column as the mobile phase was changed via a linear gradient to 20% Solvent A and 80% Solvent B over 18 min. The column was held at a constant temperature of 60 °C. The Q-TOF was operated in 2 GHz Extended Mass Range (500−5000 m/z) mode at an acquisition rate of 1 spectrum/s. The 1221.990,637 m/z ion of the HP-1221 calibration standard (part #G1982-85001, Agilent Technologies, Santa Clara, CA) was used as a reference mass throughout the run. Deconvolution of the resulting spectrum was performed using BioConfirm 8.0, using the maximum entropy algorithm. The combined uncertainty of this mass measurement is ±5 Da.

2.6. Multi angle light scattering

200 μL of 100 μmol/L filtered Fab protein was injected into a Shodex protein KW-804 column (Showa Denko America, Inc., New

York, NY) that was coupled to an Agilent 1200 HPLC system (Agilent Technologies, Santa Clara, CA), comprising a degasser, an isotropic pump, an autosampler and a variable wavelength UV detector. The running buffer was 20 mmol/L monosodium phosphate, 100 mmol/L sodium chloride, pH 7.3, with a flow rate 0.5 mL/min. A multi-angle light scattering detector (MALS), model miniDawn Treos (Wyatt Technology Corporation, Santa Barbara, CA), operating at a wavelength of 658 nm with an Optilab rEX detector (Wyatt Technology Corporation, Santa Barbara, CA), was used for molar mass determination. Astra® software version 5.3.4.14 (Wyatt Technology Corporation, Santa Barbara, CA) was used to handle signals from the detectors (MALS, differential refractive index (dRI), and UV) to compute the protein M_w and concentration values using a refractive index increment dn/dc value of 0.185 mL/g. MALS and dRI instruments were operated at 25 °C.

2.7. Crystallography

The Fab fragment was crystallized by vapor diffusion and its structure was determined by molecular replacement methods as described in Ref. [13]. Crystal growth, twinning and pseudosymmetry caused some complications, but the final structure refined well and has been deposited in the Protein Data Bank (PDB) (Ref. #9) as 5K8A. The final structure has R_{free} = 0.24; other statistics are in the PDB and in Ref. [13].

3. Results

After incubation of NISTmAb with immobilized papain and removal of the protease, the material was characterized by sodium dodecyl sulfate polyacrylamide gel electrophoresis (SDS-PAGE) in non-reducing and reducing conditions (Fig. 1). Under non-reducing conditions beta-mercaptoethanol is absent, and SDS detergent stabilizes denaturation. SDS negatively charges the proteins, but it does not break disulfide bonds. The intact disulfides prevent SDS from fully unfolding the Fab, resulting in two distinct forms of slightly different mobility. Under these non-reducing conditions the intact Fab fragment appears in the non-reduced SDS PAGE gel as a broadened double band around 50 kDa (Fig. 1A) [14]. The clarity of this double band varies with concentration (Fig. 1A, Lanes (b), (c), (e), (f)) The gel conducted under reducing conditions, which has broken the disulfide bonds between the light and heavy chains, exhibits a distinct 25 kDa band (Fig. 1B) at all concentrations (Fig. 1A, Lanes (b'), (c'), (e'), (f')).

Capillary gel electrophoresis (CGE) has proved to be an efficient and versatile approach for physicochemical characterization of

bioactive molecules. CGE is used for rapid separation of SDS protein complexes according to their molecular masses. A linear relationship exists between migration time and log molecular masses [15]. The ability of CGE to separate molecules accurately and consistently relies on a constant field strength across the capillary and the pH of the buffer solution, and ultimately, on the charge to mass ratio of the molecules [16]. Here, we used the PA 800 *plus* IgG Purity/Heterogeneity Assay (SCIEX, A10663) to complement our SEC, MALS, and mass spectrometry data, to verify the present interpretation of Fig. 1A, and to provide evidence that the Fab fragment is absent heterogeneity and impurities. Fig. 2A presents the capillary gel electrophoresis trace for the Fab fragment under reduced
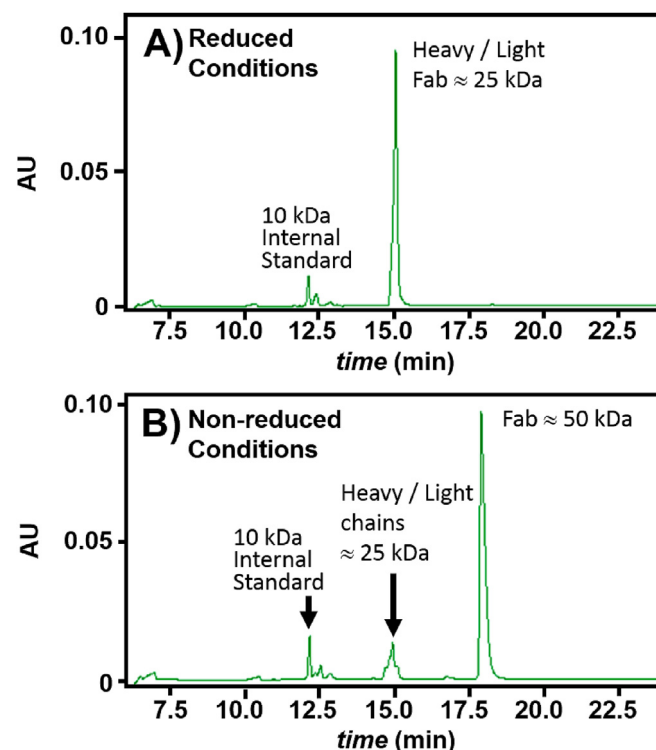

Fig. 2. Capillary Gel Electrophoresis of the Fab fragment: A) Electropherogram of the reduced Fab presents at migration time 15 min a single peak corresponding to both heavy and light chains (mass ≈ 25 kDa). B. Electropherogram of nonreduced Fab presents a predominant peak corresponding to Fab (mass ≈ 50 kDa) at migration time 18 min and a minor trace at 15 min corresponding to ≈ 25 kDa. Both electropherograms are absent evidence for other species.
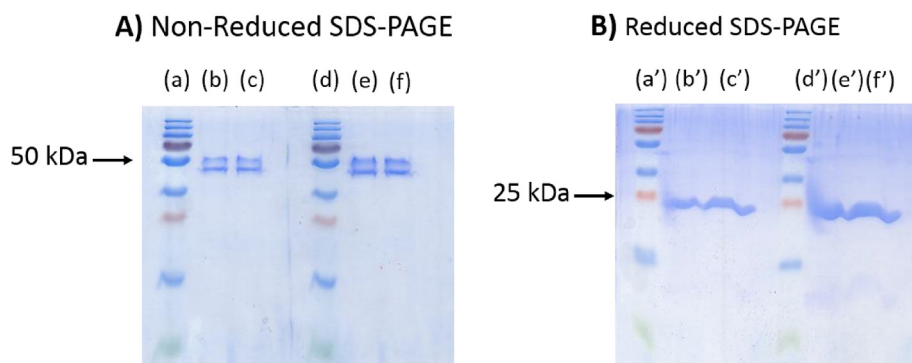

Fig. 1. SDS-PAGE analysis of different Fab fragment concentrations in non-reducing and reducing conditions. A) Non-reduced SDS-PAGE gel. Lane (a) and Lane (d) are the protein standard ladders, Lane (b) 1 µg/µL Fab, Lane (c) 1.5 µg/µL Fab, Lane (e) 2 µg/µL, Lane (f) 3 µg/µL Fab. B) Reduced SDS-PAGE gel. Lane (a') and Lane (d') are the protein standard ladders, Lane (b') 1 µg/µL Fab, Lane (c') 1.5 µg/µL Fab, Lane (e') 2 µg/µL, Lane (f') 3 µg/µL Fab.

conditions. The trace shows only one peak at 15.0 min elution time, corresponding to ≈25 kDa, which are the molecular weights of the heavy and light chains of the Fab. The minor peak around 12 min elution time is the 10 kDa internal standard. Similar profile is obtained for CGE of Fab fragment under non-reduced conditions (Fig. 2B). This trace exhibits one major peak at 18.0 min elution time, corresponding to ≈50 kDa, which is the mass of the intact Fab fragment, as this sample is not reduced. Fig. 2B exhibits a small trace at 15 min elution, indicating that a small fraction of Fab fragment has been reduced by the presence of SDS. Under both reduced and non-reduced conditions, peaks at lower or higher molecular weight are not observed, indicating the absence of impurities and aggregates.

Size exclusion chromatography then yielded Fab protein of purity better than 99% (Fig. 3A). Electrospray quadrupole time-of-flight (ESI-Q-TOF) of the size exclusion chromatography (SEC) eluent exhibited a series of $[M + nH]^{n+}$, ($n = 1, 2, 3 …$) ion peaks (not shown). Deconvolution of these peaks reduced to a synthetic [M] neutral mass spectrum of Fab fragment, evincing a species of 47,628 ($\pm$5) Da [17]. The calculated mass is 47,627 Da; hence, the mass spectrum is in accord with the calculated mass. Computation of the calculated mass requires a series of adjustments for protein modifications. Popular protein mass calculators yield the mass, 47,655 Da, by assuming the presence of a glutamate at the N-terminus and four intrachain and one interchain disulfide bonds. However, NISTmAb has a pyroglutamate (pGlu) at the N-terminus of the heavy chain, which is a frequently observed cyclization of the gene-encoded N-terminal glutamine [18–20]. Accounting for the pyroglutamate (-18 Da) and five disulfides (four intrachain and one between chains, thus, losing ten hydrogens per Fab (-10 Da) [7,21,22]. Hence, the observed and predicted mass of the Fab fragment are in accord and confirm that papain cleaves NISTmAb after CDKTH[227]. Table 1 summarizes these properties of the Fab fragment of NISTmAb. The combined uncertainty of each measurement reported in this work is one standard deviation (1σ).

Multi-angle light scattering measurements (MALS) determined the polydispersity values, $M_w/M_n = 1.004$ and $M_z/M_n = 1.007$ (Table 1), where M_n, M_w, and M_z are molecular weights determined by a number average, a mass average, and as the third moment of mass, respectively. These polydispersity values indicate that the Fab solution is substantially free (over 99%) of aggregates or oligomers. Together the SEC, ESI-Q-TOF, and MALS data imply an upper bound on all macromolecular impurities including aggregates and oligomers that is well below one half percent.

MALS and SEC measurements indicate that the Fab fragment is resistant to aggregation under stresses typical of refrigerated storage or shipping on ice. For example, to determine the feasibility for shipping samples, a 1.5 mL Eppendorf tube was filled with 500 μL of Fab solution (10 mmol/L disodium phosphate, 10 mmol/L monosodium phosphate, 150 mmol/L sodium chloride, pH 7.4, 100 μmol/L Fab, affixed sideways on a vortex platform (Vortex Genie 2, Bohemia, NY, USA), and agitated at 3200 repetitions per minute for 4 h at 23 °C. The SEC chromatography trace (Fig. 3A, upper trace) and MALS results (Table 1) were unchanged. Similar measurements indicated that Fab solutions remain unchanged when stored at −20 °C for eight months and that buffered, pH 7.4 solutions prepared from lyophilized Fab are also the same (data not shown).

The crystal structure (Protein Data Base (PDB) file 5K8A) [9] contains four independent copies of the Fab fragment, each containing the full light chain (213 aa) and heavy chain residues 1 to 223. In each Fab fragment the light chain and observed heavy chain carboxyl termini (i.e., for heavy chain, Cys 223) form a disulfide bond, the only covalent bond between light and heavy chains in the IgG1 subclass (Fig. 4). Most reported Fab structures omit this disulfide bond because it is relatively mobile, and thus, unobserved by diffraction. The mass spectrum of the crystallized Fab material indicates that heavy chain residues 224 to 227 are present in the crystal, but these residues are not observed. In the structure, the four Fab heterodimers are designated by chain identifiers LH, MV, AB, and EF. The four molecules are related by pseudo symmetry and have generally similar conformations except at crystal contacts [13]. Five cis-prolines per Fab are observed at the normal locations. Pairwise root-mean-square deviations over their alpha carbon atoms range from 0.07 nm to 0.12 nm, and the four elbow angles (relating Fv to constant domains), are 140°, 143°, 143°, and 145°, respectively [23]. The surface areas buried in the light-heavy interface are 19.24 nm², 18.43 nm², 18.68 nm², and 19.16 nm², respectively [24]. The four Fabs have different packing contacts and different surface conformations, including a few apparent contact-induced perturbations of the CDR loop main chains with magnitudes of ≈0.1 nm (Fig. 5). Main chain conformations vary significantly only for three residues; for two of these (light chain 29 and heavy 222) crystal contacts impinge; the other (heavy chain 140) is between glycines in an external loop. Over the 436 residues comprising each Fab fragment (each observed 4 times), 83 have some side chain rotamer variation among the four molecules. Most of these are surface locations where crystal contacts within 0.5 nm offer a reasonable explanation. The Fab molecule with the fewest CDR contacts, LH, is listed first in PDB file 5K8A and is used for rendering the structure below.
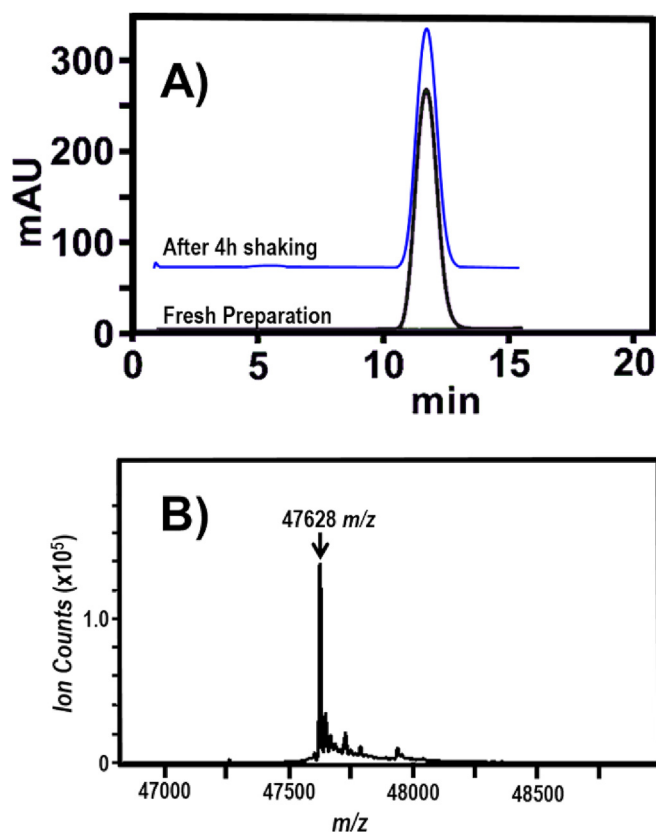

Fig. 3. SEC analysis. A) Lower trace: Size exclusion chromatograph (SEC) of freshly prepared Fab fragment (detector set at $\lambda_{abs} = 280$ nm) that displays a single eluent, corresponding to a ≈50 kDa product. Upper trace: SEC of the Fab fragment after shaking for 4 h at 23 °C on the platform of a vortex mixer (See text.). **B)** The deconvoluted electrospray quadrupole time-of-flight (ESI-Q-TOF) mass spectrum from effluent at the signal maximum of the SEC chromatography trace. Thedeconvoluted peak at 47,628 ($\pm$5) m/z, indicates a measured molecular weight for the Fab fragment of 4762 ($\pm$5) g/mol.

Table 1
Summary of measured and computed properties of the Fab fragment.

Property	Fab fragment Value	Heavy Chain Value	Light Chain Value
Formula	$C_{2114}H_{3273}N_{557}O_{667}S_{15}$	$C_{1094}H_{1701}N_{287}O_{337}S_8$	$C_{1020}H_{1574}N_{270}O_{330}S_7$
# amino acids	440	227	213
Calculated Molecular Weight (Da)	47,645[a]	24,523[b]	23,124[b]
Measured Molecular Weight (Da)	47,628 (5)[c]		
Polydispersity measured by MALS			
Fresh preparation:			
Mw/Mn	1.004		
Mz/Mn	1.007		
After 4 h agitation:			
Mw/Mn	1.004		
Mz/Mn	1.007		
FASTA Sequence	>sp|NHVY|NH_NISTmAb heavy chain AA=227 QVTLRESGPALVKPTQTLTLTCTFSGFSLSTAGMSVGWIRQPPGKALEWLADIWWDDKKHYNPSLKDRLTISKDTSKNQVVLKVTNMDPADTAT YYCARDMIFNFYFDVWGQGTTVTVSSASTKGPSVFPLAPSSKSTSGGTAALGCLVKDYFPEPVTVSWNSGALTSGVHTFPAVLQSSGLYSLS SVVTVPSSSLGTQTYICNVNHKPSNTKVDKRVEPKSCDKTH>sp|NLGT|NL_ NISTmAb light chain AA=213DIQMTQSPSTLSASVGDRVTITCSASSRVGYMHWYQQKPGKAPKLLIYDTSKLAS GVPSRFSGSGSGTEFTLTISSLQPDDFATYYCFQGSGYPFTFGGGTKVEIKRTVAAPSVFIFPPSDEQLKSGTASVVCLLNNFYPREAK VQWKVDNALQSGNSQESVTEQDSKDSTYSLSSTLTLSKADYEKHKVYACEVTHQGLSSPVTKSFNRGEC		

[a] Value accounts for intrachain disulfide bonds on the heavy and light chains and one interchain disulfide bond between heavy and light chains. The software posits a glutamate N-terminus in place of the actual pyroglutamate modification [21]. See text.
[b] Molecular weight of the free fragments based on glutamate N-terminus.
[c] 1 σ precision.

4. Discussion

NISTmAb was produced specifically to support metrology in biopharmaceutical applications, and is supported by measurements spanning over twenty-four analytical techniques [25], making it the most thoroughly characterized, publicly available, monoclonal antibody standard [4,5,7,8]. The NISTmAb can serve as an external system suitability control, help optimize measurement methods, determine instrument performance and variability, and enable comparison of changing analytical test methods for proteins in general. Moreover, because this nonproprietary reference material of known higher-order structure is publicly available [5], it is a suitable platform for experimental validation of molecular modeling studies. NISTmAb is also well suited to assist with method validation in processes focused specifically on Fab fragments. Fab from NISTmAb meets International Organization for Standardization (ISO) definitions, as specified in ISO/IEC 17,025 and ISO Guide 34 [26,27], for homogeneity, stability, and suitability for its intended measurement process.

The present crystal structure of the Fab fragment of NISTmAb provides crucial three-dimensional structural data that can support the interpretation of higher order measurements. For example, NIST has organized two ongoing studies specific to the Fab of NISTmAb. Twenty-three laboratories in ten countries are engaged in an NMR interlaboratory comparison project that uses the Fab to evaluate the reproducibility of protein NMR measurements and to validate NMR structural fingerprinting measurements for assessments of higher order structure. In another project, fifteen laboratories in four countries have conducted hydrogen-deuterium exchange mass spectrometry (HDX-MS) measurements on the Fab fragment of NISTmAb. HDX-MS measurements have become an important tool for measurements of mAb dynamics and epitope interactions [28–31]. This interlaboratory study will evaluate the reproducibility of HDX-MS measurements in chromatographically separated peptic digests of the Fab fragment. The NMR and HDX-MS studies will be published elsewhere.

To survey trends in available structural information on Fabs, Fig. 6 plots the 498 human Fab and four mammalian mAb crystal structures in the PDB database by resolution [9], release date from the PDB, and technical application. The symbol, "Y", marks the publication of four intact mammalian IgG structures (1HZH, 1IGT, 1IGY, and 5DK3) [32–35]. Solid squares represent the 164 apo-Fabs (Fabs with no bound antigen). Solid triangles represent the 275 holo-Fabs (Fab-antigen complexes). Structures associated with clinical applications, as defined by key words of "humanized" and "clinical", are marked by symbols with larger, unfilled red outlines. Of these, red unfilled triangles represent the apo-Fabs (30 structures) and red unfilled squares represent the holo-Fabs (25 structures). An unfilled oval marks the apo-Fab structure reported in this paper, 5K8A. Fig. 6 shows several trends. First, the publication rate of antibody structures has shown remarkable acceleration, as nearly half of all structures have appeared within the past 4 years. Second, the field is showing a strong trend toward study of clinically-relevant structures at high-resolution. In view of the increased study of clinical monoclonal mAbs and the structures of their Fabs, the availability of a reference mAb material with a well-described Fab may facilitate product quality assurance and research objectives.

The crystal structure 5K8A features four independent molecules of the Fab fragment in a novel packing arrangement that is described in Ref. [13]. Analysis of thermal parameters shows that the most mobile parts of all four Fabs in the crystal are not the CDR loops, which tend to be constrained by crystal packing contacts;
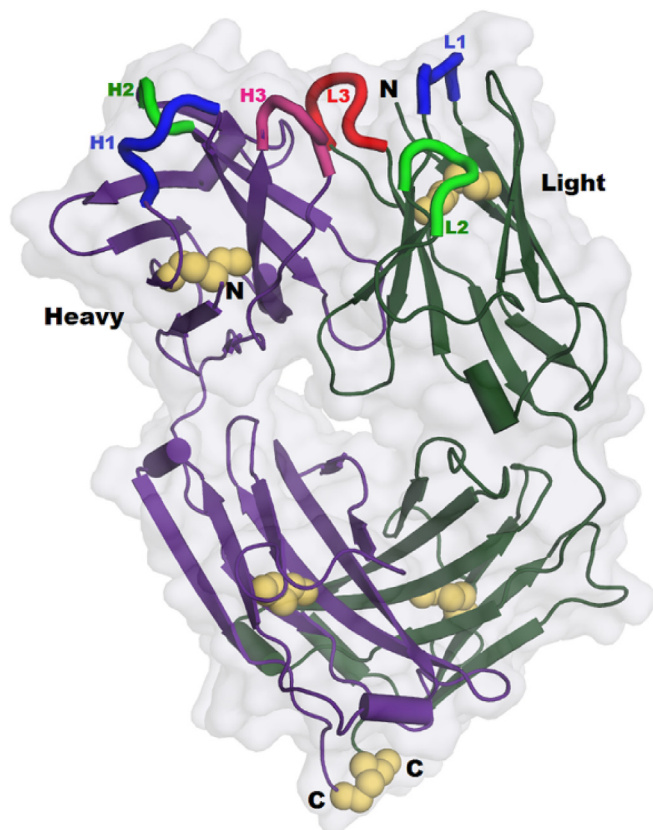
Fig. 4. Overall view of the Fab fragment (chains L and H) in PDB 5K8A. The 5 disulfides are emphasized using yellow spheres, including the sole interchain link, between the observed C-termini at bottom. Cores of the CDR loops are shown in bright colors at top. Molecular surface shows the 'hole' through the center of the Fab fragment, between the elbows. (For interpretation of the references to colour in this figure legend, the reader is referred to the web version of this article.)
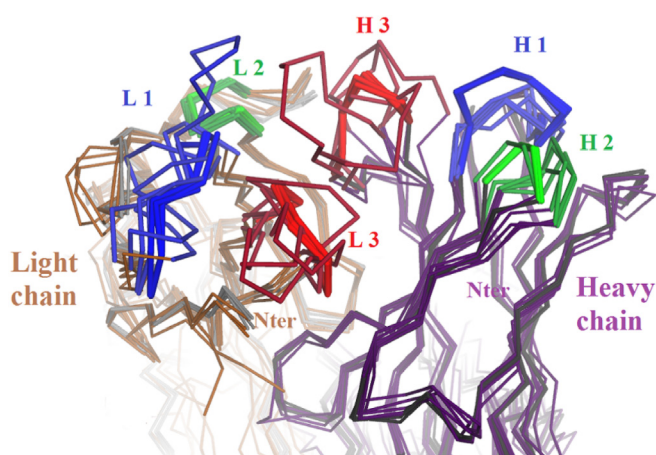

Fig. 5. Superposition of the four independent paratopes in 5K8A, along with five high-resolution precedent structures from the PDB (2VXV, 2XZA, 3N9G, 3NTC, and 4M5Y). The cores of the six CDR loops are shown in blue, green and red. Apart from the CDR loops, the mainchain conformations are all well conserved. In the CDR loops, the four structures in 5K8A are also very similar. In the CDR loops, the five precedents have not only different sequence, but different lengths, so their conformations show large variations. (For interpretation of the references to colour in this figure legend, the reader is referred to the web version of this article.)

rather, they are the C-termini (where the disulfide does not appear to confer rigidity) and two exposed loops in the heavy chain CH1 domain (loop CH1-1, residues 135 to 140, and loop CH1-5, residues

193 to 198) [13]. The CH1-1 loop has been suggested to have a functional role involving variations in antigen affinity and specificity [36]. Superposition of the present structure with its ligand-bound precedents 3QWO and 3IXT shows evidence that the CDR loops move very little on binding antigen (Fig. 7) [10]. The residue side chain that moves the most, Phe 103 of the heavy chain, appears torsionally free in the unbound state, and pressed against the antibody when bound. Two ordered water molecules appear to be displaced from the paratope by antigen binding, while several others are retained in the interface.

In order to measure the similarity of the reported 5K8A Fab structure to other human Fab fragments in the PDB, root-mean-square deviations (RMSD) were calculated over C-alpha atoms between the first molecule in 5K8A (LH) and each of the 20 highest-resolution human Fabs in the PDB. These RMSD's were calculated separately for the N-terminal half (i.e., the Fv fragment) and the C-terminal half, since for entire Fabs the elbow angle would skew the measurements. All 20 of the RMS deviations for Fv fragments are under 0.11 nm, while for the Fab C-terminal halves, RMSD's are between 0.04 and 0.16 nm. The corresponding superpositions show that the Fab C-terminal halves generally have their largest structural variations in the two heavy chain loops CH1-1 and CH1-5 mentioned above. Thus the four structures in 5K8A are generally representative of the set of known human Fab structures, reflecting conformational diversity of four distinct types: CDRs, elbow angles, the two uniquely mobile heavy chain loops CH1-1 and CH1-5, and local variations at crystal contacts.

5. Conclusion

This report presents the primary reference for the higher order structure of uncomplexed Fab fragment from the NIST Reference Antibody RM 8671. The Fab fragment of NISTmAb is a homogeneous, unglycosylated protein [37], which is straightforward to prepare, resists aggregation, and remains stable during shipping and in storage. Based on the extensive NIST experience with the Fab fragment and the availability of the parent NISTmAb, both materials are appropriate for laboratory programs that evaluate analytical instrumentation, instrument calibration, and variability in analytical test methods. For those fingerprinting methods that are particularly sensitive to the higher order structure (*e.g.*, NMR [38], hydrogen-deuterium exchange [39], covalent labeling [40]), the reported Fab reference structure provides a useful starting point for the interpretation of measurements. This nonproprietary reference material is publicly available, which makes it a suitable platform for experimental validation of molecular modeling studies. Although NIST does not currently offer the Fab fragment of NISTmAb as a reference material, the described preparation procedures can efficiently produce material with consistent quality and minimal structural variation.

Disclaimer

Certain commercial materials and equipment are identified in order to adequately specify experimental procedures. Such identifications neither imply recommendation or endorsement by the National Institute of Standards and Technology nor does it imply that the material or equipment identified is the best available for the purpose.
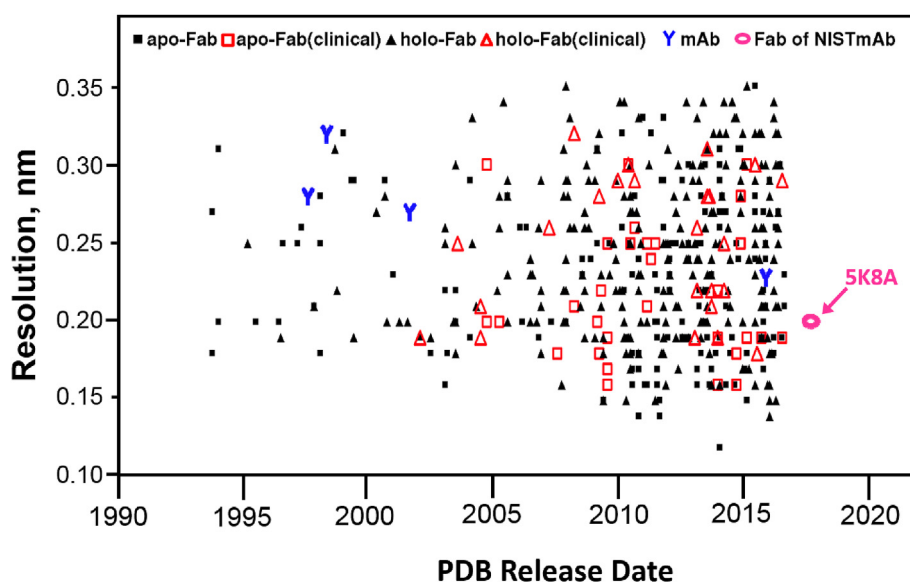
Fig. 6. PDB crystal structures plotted by their resolution, release date, and application. A total of human or humanized 494 Fab structures are included. Triangles represent apo-Fabs (Fabs with no antigen bound) while squares represent holo-Fabs (Fab-antigen complexes). Ordinary structures are represented by small solid black marks (275 black squares for the most abundant group, holo-Fabs, and 164 black triangles for apo-Fabs). Clinically relevant structures (those identified in the structure title as humanized Fabs or as derived from clinical mAbs) are emphasized by using large unfilled red triangles for apo-Fabs (30 structures) and unfilled red squares for holo-Fabs (25 structures). Also plotted are the PDB's four intact IgG antibodies (blue Y's), and the Fab fragment structure reported in this paper, 5K8A (red unfilled oval). The plot shows the acceleration of the field, with about half the structures appearing in the past four years, and a trend toward study of clinically-relevant structures at high-resolution. (For interpretation of the references to colour in this figure legend, the reader is referred to the web version of this article.)
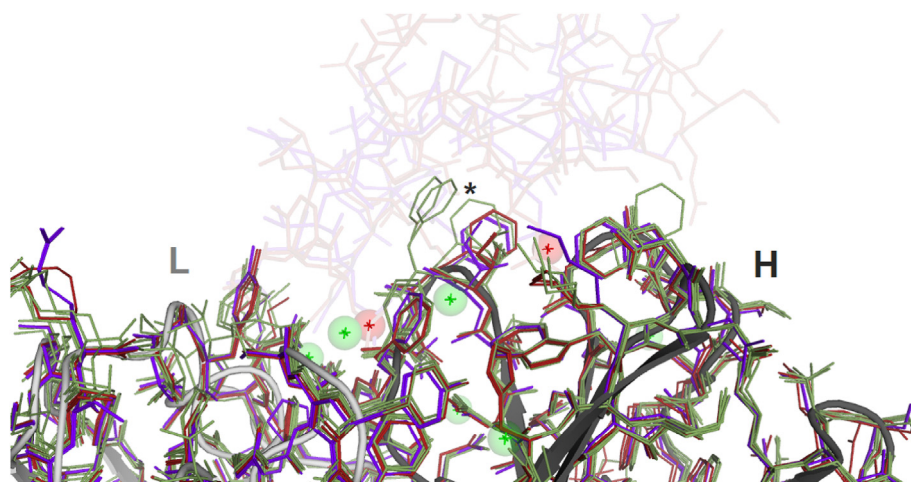

Fig. 7. Superposition of 5K8A with ligand-bound precedent structures in the paratope region. The four structures in 5K8A are shown in green, and the two previously reported ligand-bound structures are shown in purple (PDB:3IXT, resolution 0.275 nm) and dark red (PDB:3QWO, resolution 0.19 nm), with antigens rendered as transparent, at top. The view direction is similar to that in Fig. 5. The eight structures of the interface (both 3IXT and 3QWO include two independent structures) include dozens of water molecules; eight waters are shown here as spheres, using green for six that are conserved (present in both 3QWO structures and at least two of the 5K8A structures), and red for two waters that are apparently displaced from the paratope by antigen. Rearrangements are small; most CDR side chains show no significant motion, and there are no main chain shifts over 0.1 nm. The central asterisk marks Phe 103 of the heavy chain (CDR H3), which has the largest shift on binding. (For interpretation of the references to colour in this figure legend, the reader is referred to the web version of this article.)

Declaration of interest

All authors were employees of the National Institute of Standards and Technology during this work. The authors declare no conflict of interest.

Contributors

IK, ESG, DTG and JWH conceived and designed the experiments. IK, ESG, CG, and DTG performed the experiments.

Standards and Technology, a nonregulatory agency of the Department of Commerce, United States of America Federal government.

Appendix A. Supplementary data

Supplementary data related to this article can be found at https://doi.org/10.1016/j.biologicals.2017.09.005.

References

[1] Ecker DM, Jones SD, Levine HL. The therapeutic monoclonal antibody market. mAbs 2015;7:9—14.
[2] Antibodies Market worth US$ 341 Bn by 2026. [accessed 13 OCT 2016]. http://www.medgadget.com/2016/10/antibodies-market-worth-us-341-bn-by-2026.html.
[3] Liu H, Gaza-Bulseco G, Faldu D, Chumsae C, Sun J. Heterogeneity of monoclonal antibodies. J Pharm Sci;97:2426—2447.
[4] RM 8671-NISTmAb, Humanized IgG1κ Monoclonal Antibody. Gaithersburg, MD: National Institute of Standards and Technology, [accessed 12 SEP 2016]. https://www-s.nist.gov/srmors/view_detail.cfm?srm=8671.
[5] NIST Monoclonal Antibody Reference Material 8671. Gaithersburg, MD, [accessed 30 MAR 2017]. https://www.nist.gov/programs-projects/nist-monoclonal-antibody-reference-material-8671.
[6] Schiel JE, Darryl LD, Oleg VB. State-of-the-Art and emerging Technologies for therapeutic monoclonal antibody characterization volume 1. Monoclonal antibody therapeutics: structure, function, and regulatory space. In: ACS symposium series. American Chemical Society; 2014.
[7] Schiel JE, Darryl LD, Oleg VB. State-of-the-Art and emerging Technologies for therapeutic monoclonal antibody characterization volume 2. Biopharmaceutical characterization: the NISTmAb case study. In: ACS symposium series. American Chemical Society; 2015.
[8] Schiel JE, Darryl LD, Oleg VB. State-of-the-Art and emerging Technologies for therapeutic monoclonal antibody characterization volume 3. Defining the next generation of analytical and biophysical techniques. In: ACS symposium series. American Chemical Society; 2015.
[9] Berman HM, Henrick K, Nakamura H. Announcing the worldwide protein Data Bank. Nat Struct Biol 2003;10:980.
[10] McLellan JS, Correia BE, Chen M, Yang Y, Graham BS, Schief WR, et al. Design and characterization of epitope-scaffold immunogens that present the motavizumab epitope from respiratory syncytial virus. J Mol Biol 2011;409:853—66.
[11] Kaufmann B, Vogt MR, Goudsmit J, Holdaway HA, Aksyuk AA, Chipman PR, et al. Neutralization of West Nile virus by cross-linking of its surface proteins with Fab fragments of the human monoclonal antibody CR4354. PNAS 2010;107:18950—5.
[12] Michaelsen TE. Fragmentation and conformational changes of IgG subclasses. In: Shakib F, editor. The human IgG subclasses UK. Pergamon Press; 1990. p. 31.
[13] DT G IK, JW H CG. Crystal packing geometry and pseudosymmetry in the structure of the Fab fragment from the NIST reference antibody, RM 8671 Data in Brief. 2017. submitted for publication.
[14] Instructions: Pierce Fab Preparation Kit 44985. Rockford, IL USA: Pierce Biotechnology, Thermo Fisher Scientific Inc.; 2013. www.thermoscientific.com/pierce.
[15] Lausch R, Scheper T, Reif OW, Schlösser J, Fleischer J, Freitag R. Rapid capillary gel electrophoresis of proteins. J Chromatogr 1993;654:190—5.
[16] Sekhon BS. An overview of capillary electrophoresis: pharmaceutical, biopharmaceutical and biotechnology applications. J Pharm Educ Res 2011;2:2.
[17] Mann M, Meng CK, Fenn JB. Interpreting mass spectra of multiply charged ions. Anal Chem 1989;61:1702—8.
[18] Yu L, Vizel A, Huff MB, Young M, Remmele Jr RL, He B. Investigation of N-terminal glutamate cyclization of recombinant monoclonal antibody in formulation development. J Pharm Biomed Anal 2006;42:455—63.
[19] Liu YD, Goetze AM, Bass RB, Flynn GC. N-terminal glutamate to pyroglutamate conversion in vivo for human IgG2 antibodies. J Biol Chem 2011;286:11211—7.
[20] Formolo T, Ly M, Levy M, Kilpatrick L, Lute S, Phinney K, et al. Determination of the NISTmAb primary structure. In: Schiel JE, Davis DL, Borisov OV, editors. State-of-the-Art and emerging Technologies for therapeutic monoclonal antibody characterization volume 2. Biopharmaceutical characterization: the NISTmAb case study. American Chemical Society; 2015. p. 1—62.
[21] Kilpatrick E. NIST Mass and Fragment Calculator Software, ver. 1.3. Gaithersburg, MD: NIST. https://www.nist.gov/services-resources/software/nist-mass-and-fragment-calculator-software.
[22] Kilpatrick EL, Liao W-L, Camara JE, Turko IV, Bunk DM. Expression and characterization of 15N-labeled human C-reactive protein in Escherichia coli and Pichia pastoris for use in isotope-dilution mass spectrometry. Protein Expr Purif 2012;85:94—9.
[23] Stanfield RL, Zemla A, Wilson IA, Rupp B. Antibody elbow angles are influenced by their light chain class. J Mol Biol 2006;357:1566—74.
[24] Krissinel E, Henrick K. Inference of macromolecular assemblies from crystalline state. J Mol Biol 2007;372:774—97.
[25] Schiel JE, Tarlov MJ, Phinney KW, Borisov OV, Davis DL. A global partnership advancing biopharmaceutical development: summary and future perspectives. In: Schiel JE, Davis DL, Borisov OV, editors. State-of-the-Art and emerging Technologies for therapeutic monoclonal antibody characterization volume 3. Defining the next generation of analytical and biophysical techniques. American Chemical Society; 2015. p. 415—31.
[26] Panteghini M, Forest JC. Standardization in laboratory medicine: New challenges. Clin Chim Acta 2005;355:1—12.
[27] Argiriadi MA, Xiang T, Wu C, Ghayur T, Borhani DW. Unusual water-mediated antigenic recognition of the proinflammatory cytokine Interleukin-18. J Biol Chem 2009;284:24478—89.
[28] Berkowitz SA, Engen JR, Mazzeo JR, Jones GB. Analytical tools for characterizing biopharmaceuticals and the implications for biosimilars. Nat Rev Drug Discov 2012;11:527—40.
[29] Houde D, Berkowitz SA. Conformational comparability of factor IX-Fc Fusion protein, factor IX, and purified Fc fragment in the absence and presence of calcium. J Pharm Sci 2012;101:1688—700.
[30] Malito E, Faleri A, Lo Surdo P, Veggi D, Maruggi G, Grassi E, et al. Defining a protective epitope on factor H binding protein, a key meningococcal virulence factor and vaccine antigen. PNAS 2013;110:3304—9.
[31] Pirrone GF, Iacob RE, Engen JR. Applications of hydrogen/deuterium exchange MS from 2012 to 2014. Anal Chem 2015;87:99—118.
[32] Scapin G, Yang X, Prosise WW, McCoy M, Reichert P, Johnston JM, et al. Structure of full-length human anti-PD1 therapeutic IgG4 antibody pembrolizumab. Nat Struct Mol Biol 2015;22:953—8.
[33] Harris LJ, Larson SB, Hasel KW, McPherson A. Refined structure of an intact IgG2a monoclonal antibody. Biochemistry 1997;36:1581—97.
[34] Harris LJ, Skaletsky E, McPherson A. Crystallographic structure of an intact IgG1 monoclonal antibody. J Mol Biol 1998;275:861—72.
[35] Saphire EO, Parren PWHI, Pantophlet R, Zwick MB, Morris GM, Rudd PM, et al. Crystal structure of a neutralizing human IgG against HIV-1: a template for vaccine design. Science 2001;293:1155.
[36] Sela-Culang I, Alon S, Ofran Y. A systematic comparison of free and bound antibodies reveals binding-related conformational changes. J Immunol 2012;189:4890—9.
[37] Prien JM, Stöckmann H, Albrecht S, Martin SM, Varatta M, Furtado M, et al. Orthogonal Technologies for NISTmAb N-Glycan structure elucidation and quantitation. In: Schiel JE, Davis DL, Borisov OV, editors. State-of-the-Art and emerging Technologies for therapeutic monoclonal antibody characterization volume 2. Biopharmaceutical characterization: the NISTmAb case study. American Chemical Society; 2015. p. 185—235.
[38] Arbogast LW, Brinson RG, Marino JP. Mapping monoclonal antibody structure by 2D C-13 NMR at natural abundance. Anal Chem 2015;87:3556—61.
[39] Marino JP, Brinson RG, Hudgens JW, Ladner JE, Gallagher DT, Gallagher ES, et al. Emerging Technologies to assess the higher order structure of monoclonal antibodies. In: Schiel JE, Davis DL, Borisov OV, editors. State-of-the-Art and emerging Technologies for therapeutic monoclonal antibody characterization volume 3. Defining the next generation of analytical and biophysical techniques. American Chemical Society; 2015. p. 17—43.
[40] Kaur P, Kiselar J, Shi W, Yang S, Chance MR. Covalent labeling techniques for characterizing higher order structure of monoclonal antibodies. In: Schiel JE, Davis DL, Borisov OV, editors. State-of-the-Art and emerging Technologies for therapeutic monoclonal antibody characterization volume 3. Defining the next generation of analytical and biophysical techniques. American Chemical Society; 2015. p. 45—73.